NUMERICAL SIMULATION OF HEAVY ION CHARGE GENERATION AND COLLECTION DYNAMICS*

H. Dussault[a,b], J.W. Howard Jr.[a], R.C. Block[a], M.R. Pinto[c], W.J. Stapor[d], and A.R. Knudson[d]

Abstract

This paper describes a complete simulation approach to investigating the physics of heavy-ion charge generation and collection during a single event transient in a PN diode. The simulations explore the effects of different ion track models, applied biases, background dopings, and LET on the transient responses of a PN diode. The simulation results show that ion track structure and charge collection via diffusion-dominated processes play important roles in determining device transient responses. The simulations show no evidence of rapid charge collection in excess of that deposited in the device depletion region in typical funneling time frames (*i.e.*, by time to peak current or in less than 500 ps). Further, the simulations clearly show that the device transient responses are not simple functions of the ion's incident LET. The simulation results imply that future studies and experiments should consider the effects of ion track structure in addition to LET and extend transient charge collection times to insure that reported charge collection efficiencies include diffusion-dominated collection processes.

I. INTRODUCTION

Advances in microelectronic device technology have helped to create today's "systems on a chip." These complex microelectronic devices, including microprocessors and high density memories, can experience both transient and permanent errors caused by single event phenomena, including single event upset, latch up, burn out, and gate rupture. Single event phenomena result from the passage of a single, energetic particle through an electronic device. Energetic particles capable of producing single event phenomena naturally exist in the near-Earth regions of space, including the Van Allen radiation belts and in high altitude or high latitude Earth orbits.

Computer simulation of single event phenomena provides a complementary analysis method to traditional single event testing processes. System designers can use computer simulation of single event phenomena to improve device designs, assess fault tolerant design approaches, and focus experimental evaluations of device single event upset behavior by identifying appropriate test environments.

Many previous efforts in modeling single event phenomena have focused on simple analytical models [1-4, for example] or computer simulations of two- and pseudo-three-dimensional, cylindrical geometries[5-10, for example]. The simple analytical models have proven useful for assessing general trends *(e.g.*, the larger the reverse bias applied to a PN junction, the larger the peak transient current flowing through the device). These simple models, however, often provide incomplete or non-widely-applicable views of heavy ion charge collection processes. Cylindrical simulations have proven useful in evaluating the analytical models and supplementing experimental results by providing a first glimpse of the evolving device transient (*e.g.*, electric field distortions and current flow paths).

In this paper we will describe our approach to single event transient simulations and provide an analysis of our simulation results showing the importance of ion track structure and diffusion-dominated charge collection processes. Our investigations focus on using our first-order single event model to improve our understanding of the physics of charge generation and collection. Our transient simulations provide a consistent set of benchmark simulations for assessing the effects of ion track structure, changing device parameters, and LET on the transient response of a PN diode.

II. SIMULATION APPROACH

By their very nature, single event phenomena depend upon three-dimensional effects (*i.e.*, an ion track has a three-dimensional structure and practical devices do not generally have infinitely long or cylindrically-shaped structures). Although some single event geometries are amenable to two-dimensional simulations using cylindrical symmetry, an unrestricted investigation of single event phenomena requires a three-dimensional simulation capability to handle non-normal incidence of the ion or devices that are not cylindrically shaped. Only recently have full-capability, three-dimensional device simulations proven numerically and computationally tractable [11,12].

In our investigations, we have used a first-order single event model implemented in PADRE (PISCES [13] And Device REplacement) [14], a device-level simulator with both cylindrical and three-dimensional simulation capabilities. The interested reader is referred to Reference 14 for a more detailed description of PADRE's capabilities.

* Work sponsored in part by the Defense Nuclear Agency and USAF Rome Laboratory

a: At Rensselaer Polytechnic Institute, Department of Nuclear Engineering and Engineering Physics, Troy, NY 12180-3590
b: At USAF Rome Laboratory, RL/ERDA, Griffiss AFB, NY 13441
c: At AT&T Bell Laboratories, Murray Hill, NJ 07974
d: At Naval Research Laboratory, Washington, DC 20375

For our transient single event simulations, we have implemented a general model for charge generation from a particle track. The track can have a completely arbitrary spatial orientation, specified by an origin coordinate (x,y,z) and either an end coordinate (x,y,z) or a track length together with angles to the yz- and xz-planes. Ion track charge generation occurs as a result of adding a generation term in the continuity equations for electrons and holes. Electron-hole pairs are generated from the track as one of three radial distributions: uniform, Gaussian, or power law.

$$\text{Uniform:} \quad Q_1(r) = \begin{cases} Q_0 & r \le r_e \\ 0 & r > r_e \end{cases} \tag{1}$$

$$\text{Gaussian:} \quad Q_1(r) = Q_0 e^{-\frac{r^2}{\sigma^2}} \tag{2}$$

$$\text{Power Law:} \quad Q_1(r) = \begin{cases} Q_0[1+\frac{r}{\sigma}]^{-n} & r \le r_e \\ 0 & r > r_e \end{cases} \tag{3}$$

In the uniform and power law distributions, r_e defines the effective track radius. For our simulations we selected r_e as the range of the maximum energy secondary electron (*i.e.*, δ-ray) produced in that portion of the track. The power law distribution needs to be truncated to guarantee convergence of the integrals performed for the discretization of the charge generation.

The total charge density can be deposited in time in one of two ways: as either a step function (of arbitrary width t) or as a Gaussian-shaped function with peak, t_{pk}, and characteristic length, t. In reality, an ion strike generates its charge in the material very quickly - on the order of femtoseconds. For our simulations, however, we generate the ion track's charge using a 1 ps step function.

In the course of developing our first-order single event effects model, we have found that the single event transient response is very sensitive to numerical discretization. Specifically, because we can simulate non-uniform charge profiles and arbitrarily oriented trajectories, charge generation may produce discretization errors. Numerical integration, using the carrier density and charge distribution profile information, provides the charge deposited in mesh elements along the ion track. The single event model must then translate the total charge deposited in a given mesh element into a generation rate at each of the mesh element's nodes. The precision of the numerical integration scheme and the translation process provides the source of discretization error. In depositing the charge over the simulation grid, we must ensure that we deposit the correct total charge (*i.e.*, conserve charge) and that we maintain the correct spatial distribution profile without adding more grid density above that required for normal electrical transport calculations.

For example, in the case of a track structure for a 100 MeV iron (Fe) ion, the discretized charge may result in only 90 MeV worth of excess carriers generated for the single event simulation. This situation produces unacceptable conditions for accurate charge collection studies. To produce the correct initially deposited charge, we may then scale the deposited charge up to 100 MeV by multiplying the generation term at each node within the track by 1.11 (10/9). This general approach to scaling, however, may corrupt the initially specified charge distribution profile if we require too large a scaling factor. Additionally, even though we deposit the correct initial charge, we may still find the peak current and collected charge in error because of the change in the initial distribution of charge. Although the use of finer simulation meshes will reduce the differences, the finer mesh will translate into longer simulation times.

To improve the accuracy of the initial charge distributions, we have incorporated a higher order integration quadrature over the elements for the track generation term. By using a fourth or fifth order Gaussian quadrature scheme, we can keep the ion track charge discretization error to within several percent of the actual deposited charge. Since we use scaling values of only a few percent, the initial spatial distribution of charge should not dramatically change from the desired uniform, Gaussian or power law distributions.

III. SINGLE EVENT SIMULATIONS

Using our first-order single event effects model, we conducted a series of simulations to investigate the viability of the first-order model and to provide a benchmark set of simulations for investigating charge collection dynamics. At this time, we have not attempted to investigate more complex device-level effects, such as upsets in logic and memory cells. Instead, our investigations concentrated on three major "physics of charge collection" issues:

1. Does initial ion track structure affect the transient response of the device;

2. Does our first-order single event model provide an adequate basis for investigating the dynamics of changing device conditions such as substrate dopings and applied biases; and

3. Does incident LET provide an adequate basis for characterizing single event transient responses.

We selected a simple, one junction device structure for the benchmark simulations: the bulk P^+N diode in the NRL/Sandia test structures [15]. The diode is fundamentally a one-dimensional device: while it has a very shallow junction, the horizontal and lateral dimensions of the structure greatly exceed its vertical junction dimensions.

We modeled the diode using both prismatic ("true three-dimensional") and cylindrical ("pseudo-three dimensional") meshes. In order to keep simulation times as small as practical, we modeled only a portion of the diode by taking

advantage of the symmetry of the problem. We designed the meshes to provide for maximum detail through the depletion region and near the initial ion track. The diode's prismatic simulation mesh consisted of a 45 μm silicon cube with a 15 μm square P+ diffusion area. The P^+ region of the diode is doped with a Gaussian profile with a peak concentration of 10^{18} cm^{-3} and a junction depth of 0.6 μm. The N substrate region has a "default" doping level of 10^{15} cm^{-3}. The cylindrical simulations for the 100 MeV Fe and 25 MeV Cu ions used a cylinder with a 45 μm diameter, 45 μm length and a 15 μm diameter P^+ diffusion area. For the 395 MeV Cu ion, (range in silicon of 59.8 μm) we extended the cylindrical diode length to 80 μm. We placed the boundaries of the diode at least three "standard" diffusion lengths (~15 μm) from the initial ion track. Changing carrier lifetimes and diffusion conditions, however, may combine to produce substantially different diffusion lengths over the course of the transient.

We found some variations in the transient response between the prismatic and cylindrical meshes for 100 MeV Fe ion incident upon the diode with 5 volts reverse bias applied. As shown in Figure 1, the prismatic mesh resulted in a 7% larger peak current and 9% longer time to peak current than for the cylindrical mesh. Even with slightly less deposited charge in the prismatic mesh (~3% discretization error with no charge conservation scaling factor employed), the prismatic mesh resulted in more collected charge (~2%) than did the cylindrical mesh.

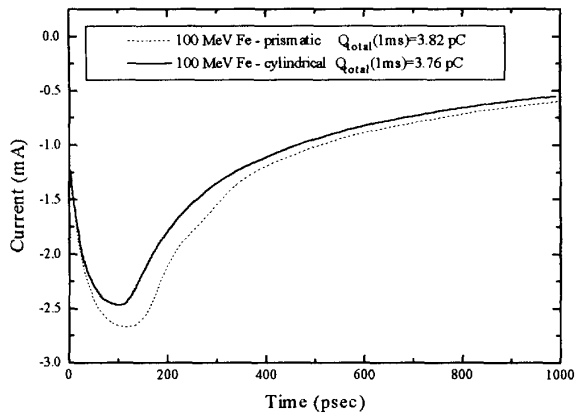

Figure 1. Prismatic and Cylindrical Mesh Simulations

Differences in circular versus rectangular structures and contacts may explain some of the differences between the two transient simulations. Our simulation meshes did result in non-infinite (*i.e.*, not truly one-dimensional) simulation structures and different total substrate resistances. These conditions may have also contributed to the differences between the cylindrical and prismatic simulations.

Since the transient simulations with the prismatic mesh required at least an order of magnitude longer computation times than the cylindrical mesh simulations, we elected to conduct our basic investigations of charge collection dynamics using the cylindrical diode geometry. Compared to a complete, three-dimensional treatment of the transient, the cylindrical mesh will provide estimates of total charge collected, peak currents, and time to peak currents. We expect, however, that these changes will be consistently reproduced for the different diode simulation conditions (*e.g.*, changing applied biases and substrate dopings). Therefore, we expect that different transient responses obtained for different diode conditions will be principally affected by different charge collection processes and not by three-dimensional simulation effects.

The following investigations of ion track structure, basic charge collection mechanisms and ions of different energy but same LET have all been undertaken using the cylindrical simulation mesh. The cylindrical mesh contains 6840 elements with 3542 grid points. Grid spacing ranges from 0.01 μm near the depletion region boundaries and initial track radius to a maximum spacing of 7.67 μm near the outer edges of the diode substrate. The mesh contains no obtuse elements. The diode simulation includes no external lumped resistances, capacitances or inductances. Physical models used in the simulations include field and concentration dependent mobility models and Shockley-Read-Hall and Auger recombination models. We assume that device temperature maintains a constant 300 ^{o}K. We enforced charge conservation for all cylindrical simulations (*i.e.*, 100 MeV Fe created ~4.4 pC of charge in the device). Transient simulations went from pre-ion-strike conditions out to one full millisecond. In all instances, the diode had completely recovered to its pre-ion-strike conditions by 1 ms.

A. Ion Track Structure

Ongoing research into ion track structure has produced many different track models[16-20]. From a physics viewpoint, one of the strongest ion track models allows LET to vary along the length of the track, has a radial distribution of excess carriers expressed by a power law distribution (based upon expressions for the range of an energetic electron in matter) with a cut-off range equal to the range of the maximum energy δ-ray produced at that depth of the ion track. We call this model, based upon Katz theory [16] and previous work by Stapor and McDonald [17], the "non-uniform power law" track model. (Equation (3) in the previous section of this paper defines the power law relationship.) But given the attractiveness and simplicity of other models, especially constant radius, uniform charge density columnar models, we first examined how important ion track structure is to charge collection dynamics.

As shown in Figure 2, different models of ion track structure can affect the transient response to a 100 MeV Fe ion incident upon the P^+N diode with 5 volts applied reverse bias. The largest effect in the track structure for the 100 MeV Fe ion appears to be the changing charge densities along the track (*i.e.*, allowing LET to change along the track).

As shown in Figure 3, more subtle differences exist among the 0.1 μm radius non-uniform track, the Gaussian distributions, and the power law distributions. For the 100 MeV Fe ion simulations, the differences between the Gaussian and power law tracks are generally within 1 - 8% of each other. In part, the similarities among the 0.1 μm radius non-uniform track, the Gaussian distributions, and the power law track models may result from the selection of a 100 MeV Fe ion that produces a track with an "average" radius of ~0.1 μm. Using the carrier concentration profiles from Katz theory, as developed by Stapor and McDonald [17], Gaussian fits to these profiles can underestimate the track centerline concentrations by one to two orders of magnitude or seriously underestimate the extent of the track radius (using a more accurate estimate of track centerline concentration results in the "near centerline Gaussian" model). Since we did not include carrier-to-carrier scattering models in our simulations, our ion track simulations probably do not completely represent the effects of Auger recombination and "plasma screening." The absence of carrier-to-carrier scattering mobility models in our simulations may have obscured even more important differences between the track models.

Our simulations do indicate that different ion track charge generation distributions can affect the device transient response. The 5 - 20% variations in key single event transient parameters (peak current, time to peak current, and collected charge) shown in our simulations for the 100 MeV Fe ion passing through a single, shallow junction provide reasonably strong evidence that track structure can play a significant role in determining charge collection dynamics. While we would expect 5 - 20 % variations in experimentally collected data, we should not accept the unnecessary introduction of such variances in our simulation of single events. We would further expect that track structure effects are even more important for higher energy ions, such as typical components of cosmic radiation, and in small geometry, closely spaced semiconductor devices such as those typically found in modern CMOS microcircuits.

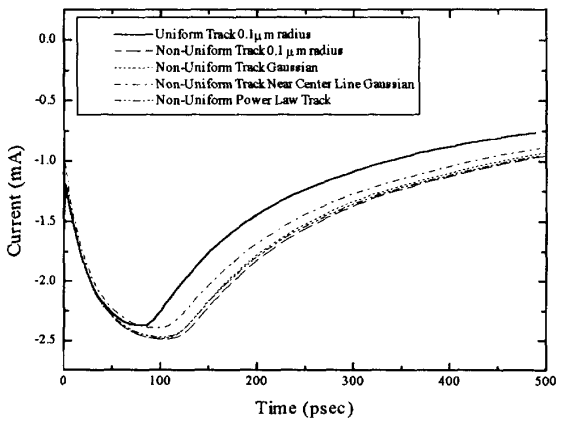

Figure 2. 100 MeV Fe Ion Track Transient Responses

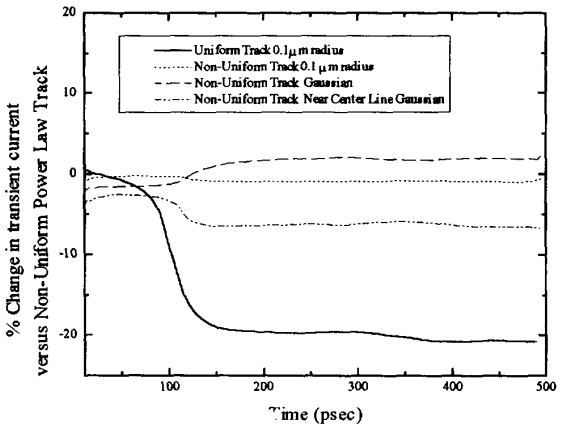

Figure 3. Relative Changes in Track Models

As a minimum, accurate ion track simulation models should include consideration of changing LET along the track length and a reasonable estimate of the changing radial extent of the ion track along its length. Based upon our simulation results and our assessment of the physics of charged particle track formation using Katz theory [16], we would recommend the use of the non-uniform power law track model for single event simulations.

B. Basic Charge Collection Mechanisms and Device Physics

In addition to investigating ion track structure effects, we examined the effects of changing some basic semiconductor parameters to evaluate our first-order single event model and to investigate the basic physics of charge collection. Our simulations have focused upon ion species and device parametric changes typically found in previously reported heavy-ion experiments [21-23].

Figure 4 shows the transient current responses for the first nanosecond of the 100 MeV Fe ion single event transient for the same non-uniform power law ion track model in the diode with 5,10 and 20 volts applied reverse bias. The transient waveforms show the expected trend of increasing peak current with increasing bias. The transient currents increase from 2.47 to 3.86 to 5.6 mA for 5, 10, and 20 volts reverse bias, respectively. The time to peak current consistently decreases with increasing bias, decreasing from 104.3 to 56.5 to 36.9 ps for 5, 10, and 20 volts reverse bias, respectively. Additionally, the increasing reverse bias produces a much sharper peak response and a shorter signal fall time. Wagner, *et al*, [23] reported similar signal rise time dependencies for 18 MeV Si and 100 MeV Fe ion experiments. Inductive limits of the equipment used in these experiments, however, may have also contributed to picosecond differences in signal rise times.

Our simulation results show that electric-field-assisted charge collection (*i.e.*, drift) and "plasma screening" effects [3] within the diode constitute the principal physical

processes contributing to the increasing peak currents and decreasing times to peak currents for increasing reverse biases. Increasing depletion layer width and increasing electric field strength combine to produce a larger current with a faster rise time. The wider depletion region provides a larger region where drift processes quickly collected the deposited charge. The larger the charge deposited in the depletion region, the larger the expected peak current. Similarly, the stronger electric field in the depletion region, the quicker the field will penetrate the dense regions of charge in the ion track where drift processes can collect the charge. Therefore, the stronger the electric field, the faster the rise time to peak current.

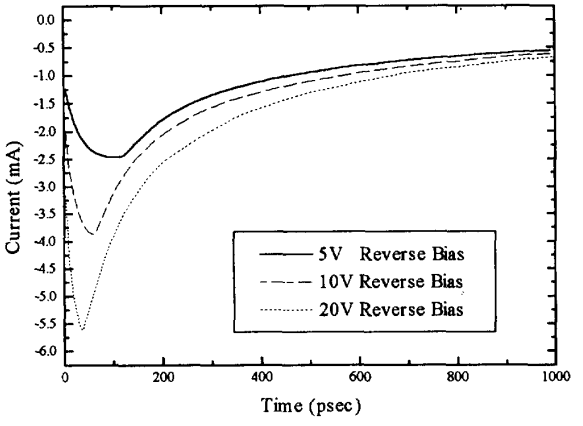

Figure 4. Responses to Changing Substrate Bias

Our simulations of the effect of changing substrate doping while keeping a constant 5 volts reverse bias during the 100 MeV Fe transient produced several interesting results. As shown in Figure 5, changes in substrate doping levels alter the overall shape of the transient response. For low substrate doping levels, the current peaks almost instantaneously. In fact, the current peaks before the 1 ps of charge generation completes. While not evident from the figure, the transient response for the 10^{14} cm^{-3} substrate doping case has a very fast rise time to the peak current, followed by a much slower "secondary pulse" peaking at approximately 1000 ps. The shape of the transient response indicates that the ion track has completely disturbed the diode's depletion region.

In our simulations, the peak currents consistently increase for increased substrate doping. The transient peak currents increased from 1.64 to 2.47 to 4.98 mA for the 10^{14}, 10^{15}, and 10^{16} cm^{-3} substrate dopings, respectively. Previously reported experimental results, however, have not shown either the very fast rise times for low substrate dopings or a consistent trend to changes in peak current levels as a function of substrate doping. Heileman, *et al* [21] reported decreasing peak currents with increasing substrate dopings for low energy alpha and boron ions. Data from 5 MeV alpha particles [23], however, indicate that peak currents may increase, decrease, or stay approximately the same depending upon substrate doping and applied biases. Additional data from Wagner, *et al*, show decreasing peak currents with increasing substrate resistivities for 18 MeV Si and 100 MeV Fe ions [23]. Heileman, *et al*, suggest that peak currents should decrease with increasing substrate doping because the depletion region is smaller and the electric field is stronger than for lower substrate doping cases [21]. Our results indicate that electric field strength provides at least as important an effect on peak transient current as does depletion region width and charge deposited in the depletion region.

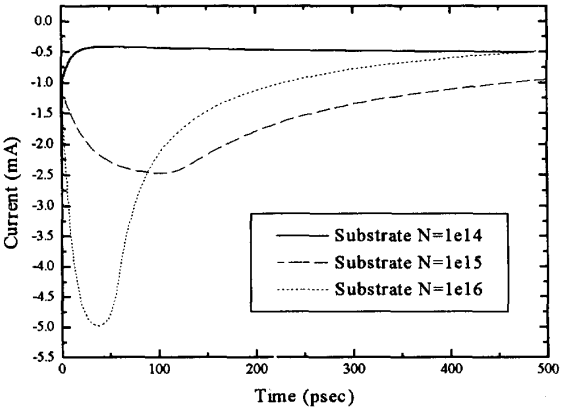

Figure 5. Responses to Changing Substrate Doping

Examining the physics of charge collection provides one clue to assessing how changing substrate doping levels impacts the dynamics of the single event transient response. We would expect that the total collected charge should decrease with increasing substrate doping. The shrinking size of the depletion region with increasing substrate doping should effectively reduce the total collected charge.

As indicated in Figure 6, our simulations show decreasing total collected charge with increasing substrate doping. The transient behavior of the charge collection, however, provides additional insight into the physics of the charge collection process. As substrate doping increases, the diode collects a larger amount of charge during the early (< 0.2 ns) portion of the transient. These results demonstrate the importance of charge collection via drift processes for diodes with high substrate dopings, while showing the importance of charge collection via diffusion processes for diodes with low substrate dopings. Additionally, these results indicate that experimentally obtained charge collection data should use long enough charge collection time constants (*i.e.*, on the order of several microseconds) to assure that the data include the contribution of charge collection via diffusion.

The McLean-Oldham model [2] suggests that the total collected charge should be proportional to $N_d^{-1/3}$. Our simulations, however, indicate a weaker relationship between substrate doping and total collected charge. The total collected charge does not decrease as rapidly as the McLean-

Oldham model predicts. The significant contribution of diffusion processes to total charge collection, as witnessed by the significant fraction of total charge collected in time frames greater than 1 ns in Figure 6, can explain the major differences in our simulation results and the McLean-Oldham model.

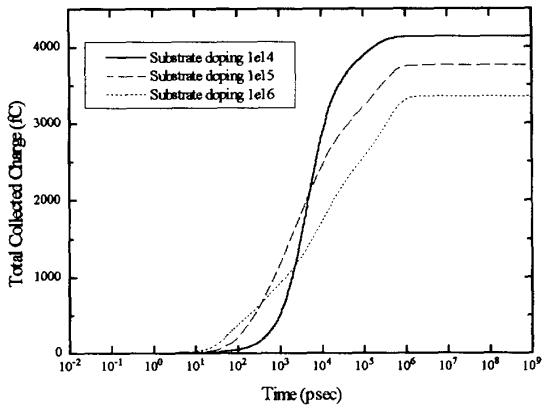

Figure 6. Charge as a Function of Substrate Doping

C. Ions of Different Energy but Same LET

Based upon our simulation results showing the importance of charge collection via diffusion-dominated processes, we investigated the transient response to ions with the same incident LET but different energies. Incident LET currently provides the basis for most reported single event susceptibility measurements in devices. Previous work has suggested that we need to reconsider measuring single event upset cross sections simply as a function of incident LET [24]. Comparing two ions of the same species and same incident LET but on different sides of the Bragg peak provides a simple means to examine using incident LET as a basis for reporting single event test results.

For our investigation of the effect of incident LET, we have selected to simulate the transient responses to a 25 MeV and 395 MeV copper (Cu) ion. Both ions have approximately the same incident stopping powers in silicon (~ 26 MeV/mg/cm^2). The 25 MeV ion has a range in silicon of 7.2 μm, and the 395 MeV ion has a range of 59.8 μm. We simulated the bulk P^+N diode response with 5 volts reverse bias applied and a substrate doping of 10^{15} cm^{-3}. As shown in Figure 7, the two copper ions produce different peak currents, time to peak currents and total collected charge. It should be noted that these effects are noticeable even for this single junction device where the junction area is reasonably close to the beginning of both ion tracks. These results imply that both transient currents and charge collection can be affected by charge deposition occurring at distances reasonably far removed from the device junctions.

The transient current peaks for the 25 MeV Cu ion at 1.69 mA and peaks for the 395 MeV Cu ion at 2.36 mA. The ~30% increase in charge deposited in the depletion region of the device by the 395 MeV Cu ion accounts for part of the ~40% increase in peak current over that for the 25 MeV Cu ion. Differences in initial electric field strength or substrate dopings should not contribute to increases in the peak current - since these values do not change in the simulations. The increase in peak current, therefore, appears attributable to other track structure effects and depletion layer transients occurring in the 395 MeV Cu case during the first 100 ps of the transient.

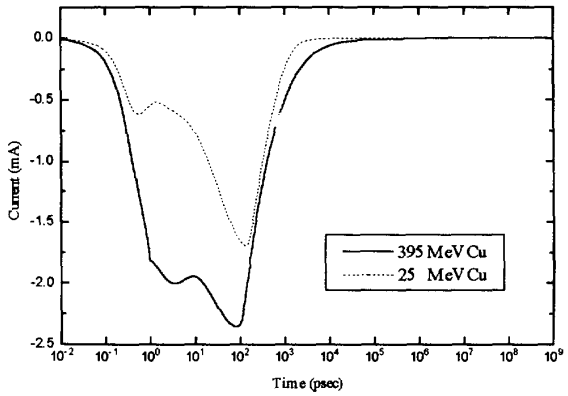

Figure 7. Responses to 25 and 395 MeV Cu Ions

The two ions also have different times to peak current. The larger radius of the 395 MeV Cu ion track (δ-ray ranges are much larger for the 395 MeV ion) can explain the smaller time to peak current for the 395 MeV Cu ion. The effective track radius in the depletion region of the device changes from ~0.02 μm for the 25 MeV ion to ~1.6 μm for the 395 MeV ion. The significantly larger effective track radius will produce a lower carrier concentration that the external electric field can penetrate much sooner than for the track with higher carrier concentrations, allowing drift-dominated processes to more quickly collect the charge.

In Figure 7, we have shown the complete transient current wave forms for our simulations on a semi-log plot. (The other transient current responses have shown only the first 500-1000 ps of transient response.) This figure shows that the transient current response is a complex function and not a simple pulsed response. We do not think that the first, early peak is a direct artifact of our numerical computation methods. Instead, the small pulse early in the transient may be the result of "plasma delay" [18,25] (*i.e.*, the time required for the external electric field to penetrate the ion track and begin drift assisted charge collection). The small pulse may arise from the step generation of charge in the ion track. During the first few tenths of a picosecond, drift-dominated collection processes cause the current to increase. But once sufficient charge density is deposited in the ion track, the "plasma screening" effect shields the deposited charge from collection, and the transient current decreases. The ion track charge density then slowly decreases as a result of ambipolar diffusion processes until the electric field in the

depletion region can once again penetrate into the charge column and resume charge collection. The current then increases to its peak value in the second pulse. Previous experiments have not reported observing this complex transient waveform, but the first peak does pass faster than signal rise times in most transient measurement equipment. Additionally, in reality, the ion deposits its charge in the semiconductor much more quickly than the 1 ps step deposition pulse used in our simulations. Therefore, we may not experimentally see the initial small pulse.

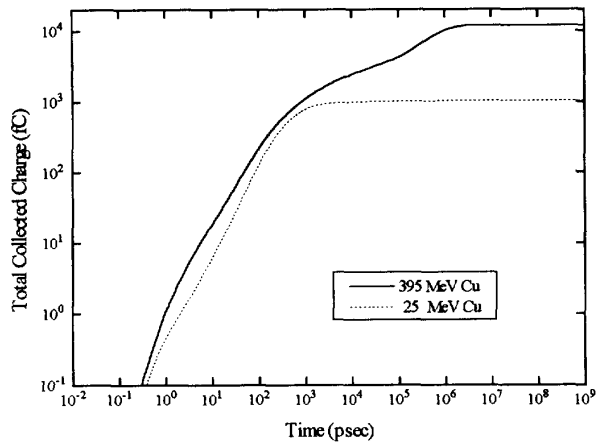

Figure 8. Charge Collection for 25 and 395 MeV Cu Ions

As shown in Figure 8, the charge collection responses for the two copper ions indicate that the relative importance of the various charge collection mechanisms are different for the two ions. In the case of the 25 MeV Cu ion, drift-dominated processes appear to collect the majority of the deposited charge. Since almost half of the charge created by the 25 MeV Cu ion has been deposited within the depletion region, we would expect that drift processes should dominate the charge collection processes. In the case of the 395 MeV Cu ion, however, diffusion-related charge collection processes appear to make a substantial contribution to overall charge collection. During the first 1 ns of the transient (a generous upper bound on drift-assisted charge collection time) both ions produce approximately the same total collected charge. This result indicates that some process other than "charge funneling" is contributing to the differences in charge collection.

In heavy-ion experiments, we should not expect to see ions with the same LET producing the same transient behavior in the device unless the effective charge collection time in the device (*e.g.*, cycle time) is under 1 ns. Single event experiments should, therefore, insure that measured charge collection efficiencies include the contribution of diffusion-dominated collection processes and should consider ion track structure effects when interpreting results.

D. Charge Collection Dynamics

Integrating the current transient responses over time produces a charge collection curve. The charge collection curve provides a useful overall picture of the dynamics of charge collection during a single event transient. A designer can use the charge collection curves to help assess single event susceptibilities and select appropriate heavy-ion test environments and conditions. For example, if the designer knows the critical charge and the device switching frequency, the curves will indicate if a given ion can deposit the critical charge in sufficiently short time to produce an upset.

The charge collection curves also provide insight into the processes involved in each portion of the heavy-ion induced transient. As shown in Figure 9, the $P^{+}N$ diode response to the 100 MeV Fe ion shows a relatively quick, drift-dominated charge collection period, ending approximately at the time of peak transient current. At times greater than 1 ns, the charge collection process switches to a slower, diffusion-dominated charge collection period. Finally, the transient completes with an even slower diffusion-dominated charge collection period reflecting the change in carrier lifetimes from high-level-injection to low-level-injection lifetimes.

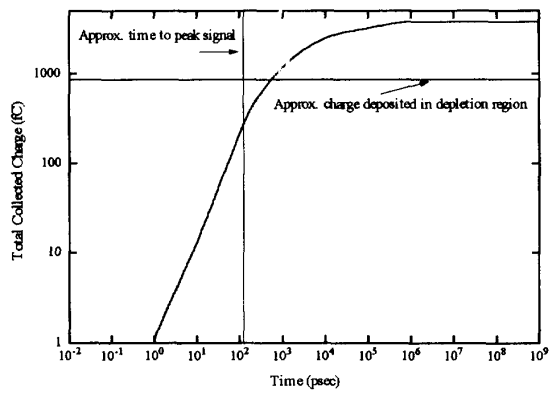

Figure 9. Charge Collection for 100 MeV Fe Ion in PN Diode

Our charge collection curves also indicate that currently used assumptions about funneling need to be reexamined. As shown in Figure 9, the simulations show no evidence of rapid charge collection in excess of that deposited in the device depletion region in typical funneling time frames (*i.e.*, by time to peak current [21] or in under 500 ps). As shown in the charge collection curve for the 100 MeV Fe ion, the total collected charge at the time of peak current is less than the charge deposited in the depletion region. Approximately 600 ps pass before the diode structure collects the charge initially deposited within the depletion region The total collected charge does, however, eventually increase beyond that charge initially deposited in the depletion region, indicating the occurrence of some "funnel-like" process. Based upon these simulation results, it appears that we need to reconsider the time scales and principal charge collection processes involved with electric field/depletion layer transients.

The simulations reported in this work provide basic insights into the charge collection dynamics associated with a heavy-ion-induced single event transient. The single event transient results reported here have not included the effects of carrier-to-carrier scattering in the simulations. We would expect that carrier-to-carrier scattering effects may produce reasonably large impacts on peak currents and recombination losses during the transient. In addition, we need to further assess the relative contributions from drift, "funneling" and diffusion processes during the single event transient.

IV. CONCLUSIONS

Numerical simulation of single events using an accurate ion track charge distribution profile allows us to investigate the fundamental processes ongoing during the transient. Our simulation results have demonstrated that ion track structure can play an important role in determining device transient behavior. Accurate models of ion track structure should allow LET to change along the track length and should provide reasonable representations of changing effective radii along track length.

Our results demonstrate that diffusion-dominated charge collection processes represent an important part of the total collected charge and overall transient response of a junction. As expected, our simulations have shown that increasing reverse bias on a junction or decreasing substrate doping increases the total collected charge, but our simulations have also provided additional insights into the processes responsible for charge collection. Additionally, our results indicate that we need to reconsider the basic processes and time frames attributed to "funneling" of charge.

Our results also have direct applicability to future heavy-ion experimental work. Charge collection resulting from diffusion-dominated processes occurs over relatively long time frames, and we should insure that measured charge collection efficiencies include the diffusion driven portions of the transient. Further, our simulations suggest that LET should not provide the only parameter directly related to the heavy- ion used in assessing single event effects. Total deposited charge and ion track structure also define important parameters in determining the transient response of a device.

In the future, we plan to explore the physics of single events with additional fully-three-dimensional simulations to examine the effects of angled ion trajectories and ion trajectories passing near or through edges of the depletion region of the P^+N diode. Additionally, we plan to examine charge collection dynamics in diodes and bipolar transistors on epitaxial layers and on insulating substrates.

V. REFERENCES

[1] C. Hu, "Alpha-Particle-Induced Field and Enhanced Collection of Carriers," *IEEE Electron Device Letters* **EDL-3**, pp 31-34 (1982).

[2] F. B. McLean and T.R. Oldham, "Charge Funneling in N- and P-Type Si Substrates," *IEEE Transactions on Nuclear Science* **NS-29**, pp 2018-2023 (1982).

[3] R.M. Gilbert, G.K. Ovrebo, and J. Schifano, "Plasma Screening of Funnel Fields," *IEEE Transactions on Nuclear Science* **NS-32**, pp 4098-4103 (1985).

[4] L.D. Edmonds, "A Simple Estimate of Funneling-Assisted Charge Collection," *IEEE Transactions on Nuclear Science* **NS-38**, pp 828-833 (1991).

[5] J.S. Fu, C.L. Axness, and H.T. Weaver, "Two-Dimensional Simulation of Single Event Induced Bipolar Current in CMOS Structures," *IEEE Transactions on Nuclear Science* **NS-31**, pp 1155-1160 (1984).

[6] H.L. Grubin, J.P. Kreskovsky, and B.C. Weinberg, "Numerical Studies of Charge Collection and Funneling in Silicon Device," *IEEE Transactions on Nuclear Science* **NS-31**, pp 1161-1166 (1984).

[7] J.G. Rollins, T.K. Tsubota, W.A. Kolasinski, N.F. Haddad, L. Rockett, M. Cerrila, and W.B. Hennley, "Cost-Effective Numerical Simulation of SEU," *IEEE Transactions on Nuclear Science* **NS-35**, pp 1608-1612 (1988).

[8] J.A. Zoutendyk, H.R. Schwartz, and L.R. Nevill, "Lateral Charge Transport from Heavy-Ion Tracks in Integrated Circuit Chips," *IEEE Transactions on Nuclear Science* **NS-35**, pp 1644-1647 (1988).

[9] A. Michez, G. Bordure, Y. Patin, and G. Gosselin, "^{4}He, ^{12}C, and ^{63}Cu Ions Effect Simulation on Silicon Diode," RADECS 91 (IEEE Press, La Grande-Motte, France, 1991), pp 419-423 (1991).

[10] A.R. Knudson and A.B. Campbell, "Comparison of Experimental Charge Collection Waveforms with PISCES Calculations," *IEEE Transactions on Nuclear Science* **NS-38**, pp 1540-1545 (1991).

[11] J.G. Rollins, "Heavy Ion Induced Latch-Up Simulation," TMA 8th Annual TCAD Seminar, Techmart Meeting Center, Santa Clara, CA, August 9, 1990.

[12] H. Iwata and T. Ohzone, "Numerical Analysis of Alpha-Particle-Induced Soft Errors in SOI MOS Devices," *IEEE Transactions on Electron Devices* **ED-39**, pp 1184-1190 (1992).

[13] M.R. Pinto, C.S. Rafferty, and R.W. Dutton, *PISCES II: Poisson and Continuity Equation Solver and Supplementary Report* (Stanford Electronics Laboratory Report, Palo Alto, 1984).

[14] M.R. Pinto, *PADRE Version 2.3 User's Manual*, (AT&T Bell Laboratories, 1992).

[15] A.B. Campbell, A.R. Knudson, P. Shapiro, D.O. Patterson, and L.E. Seiberling, "Charge Collection in Test Structures," *IEEE Transactions on Nuclear Science* **NS-30**, pp 4486-4492 (1983).

[16] E.J. Kobetich and R. Katz, "Energy Deposition by Electron Beams and δ Rays," *Physical Review* **170**, pp 391-396 (1968).

[17] W.J. Stapor and P.T. McDonald, "Practical approach to ion track energy distribution," *Journal of Applied Physics* **64**, pp 4430-4434 (1988).

[18] I. Kanno, "Models of formation and erosion of a plasma column in a silicon surface-barrier detector," *Rev. Sci. Instrum.* **58**, pp 1926-1932 (1987).

[19] M.J. Pruppers, H.P. Leenhouts, and K.H. Chadwick, "A Track Structure Model for the Spatial Energy Deposition of Ionising Radiation," *Radiation Protection Dosimetry* **31**, pp 185-188 (1990).

[20] R.C. Martin, N.M. Ghoniem, Y. Song, and J.S. Cable, "The Size Effect of Ion Charge Tracks on Single Event Multiple-Bit Upset," *IEEE Transactions on Nuclear Science* **NS-34**, pp 1305-1309 (1987).

[21] S.J. Heileman, W.R. Eisenstadt, R.M. Fox, R.S. Wagner, N. Bordes, and J.M. Bradley, "CMOS VLSI Single Event Transient Characterization," *IEEE Transactions on Nuclear Science* **NS-36**, pp 2287-2291 (1989).

[22] A.R. Knudson, A.B. Campbell, P. Shapiro, W.J. Stapor, E.A. Wolicki, E.L. Petersen, S.E. Diehl-Nagle, J. Hauser, and P.V. Dressendorfer, "Charge Collection in Multilayer Structures," *IEEE Transactions on Nuclear Science* **NS-31**, pp 1149-1154 (1984).

[23] R.S. Wagner, N. Bordes, J.M. Bradley, C.J. Maggiore, A.R. Knudson, and A.B. Campbell, "Alpha- Boron- Silicon- and Iron-Ion-Induced Current Transients in Low-Capacitance Silicon and GaAs Diodes," *IEEE Transactions on Nuclear Science* **NS-35**, pp 1578-1584 (1988).

[24]W.J. Stapor, P.T. McDonald, A.R. Knudson, A.B. Campbell, and B.G. Glagola, "Charge Collection in Silicon for Ions of Different Energy but Same Linear Energy Transfer (LET)," *IEEE Transactions on Nuclear Science* **NS-35**, pp 1585-1590 (1988).

[25]P.A. Tove and W. Seibt, "Plasma Effects in Semiconductor Devices, " *Semiconductor Nuclear-Particle Detectors and Circuits* Publication 1593, National Academy of Sciences, pp 71-78 (1969).